University of Texas Rio Grande Valley
ScholarWorks @ UTRGV

Theses and Dissertations

12-2021

Electrospun PCL and PCL/Gel Microfiber Scaffolds as Prototypes for Anterior Cruciate Ligament (ACL) Regeneration and Repair

Diego Rivera
The University of Texas Rio Grande Valley

Follow this and additional works at: https://scholarworks.utrgv.edu/etd

 Part of the Chemistry Commons

Recommended Citation

Rivera, Diego, "Electrospun PCL and PCL/Gel Microfiber Scaffolds as Prototypes for Anterior Cruciate Ligament (ACL) Regeneration and Repair" (2021). *Theses and Dissertations*. 949.
https://scholarworks.utrgv.edu/etd/949

This Thesis is brought to you for free and open access by ScholarWorks @ UTRGV. It has been accepted for inclusion in Theses and Dissertations by an authorized administrator of ScholarWorks @ UTRGV. For more information, please contact justin.white@utrgv.edu, william.flores01@utrgv.edu.

ELECTROSPUN PCL AND PCL/GEL MICROFIBER SCAFFOLDS AS PROTOTYPES FOR ANTERIOR CRUCIATE LIGAMENT (ACL) REGENERATION AND REPAIR

A Thesis

by

DIEGO RIVERA

Submitted In Partial Fulfillment of the

Requirements for the Degree of

MASTER OF SCIENCE

Major Subject: Chemistry

The University of Texas Rio Grande Valley

December 2021

ELECTROSPUN PCL AND PCL/GEL MICROFIBER SCAFFOLDS AS PROTOTYPES FOR ANTERIOR CRUCIATE LIGAMENT (ACL) REGENERATION AND REPAIR

A Thesis

by

DIEGO RIVERA

COMMITTEE MEMBERS

Dr. Javier Macossay-Torres

Chair of Committee

Dr. Hassan Ahmad

Committee Member

Dr. Debasish Bandyopadhyay

Committee Member

December 2021

Copyright 2021 Diego Rivera

All Rights Reserved

ABSTRACT

Rivera, Diego, Electrospun PCL and PCL/Gel microfiber scaffolds as prototypes for anterior cruciate ligament (ACL) regeneration and repair. Master of Science (MS), December 2021, 43 pp., 8 tables, 14 figures, 44 references, 25 titles

Polycaprolactone (PCL) is a polymer that has been a focus of tissue engineering due to its range of applicability for biomedical applications. Synthesis of PCL from a microwave-assisted and stannous octoate-catalyzed ring-opening reaction with ε-caprolactone was accomplished. Aligned-fiber microfiber mats were generated via electrospinning for characterization. PCL microfiber mats were characterized via FTIR and scanning electron microscopy. These PCL microfiber mats were mechanically tested to examine their applicability as tools for knee ligament repair. During tensile testing, non-fiber aligned mats lacked the sufficient elastic modulus. Fiber-aligned PCL samples both and gelatin-coated were tested and showed enhanced elastic modulus and extension at break point. Braiding gel-coated PCL samples failed due to splintering caused by drying of gelatin on scaffold surface. Biodegradation testing was carried out using phosphate buffered saline, elastase, and MMP-1 collagenase to simulate synovial fluid. Gel-coated PCL scaffolds showed consistent degradation with loss of mass no more than 22%.

DEDICATION

My thesis work and other academic achievements are dedicated, with immense gratitude, to my family and friends. I wish to thank my mother, Maria Rivera, and my father, Humberto Rivera, for their care and support throughout my time in university. Your love, unfailing encouragement, and guidance helped me to continue striving forward and are the reason I am here today. I also want to thank my sister Gabby for all the love and guidance she has provided throughout my life. Thank you for always being there for me and for making difficult times easier with nothing more than your company. I want to thank my friends Obed, Dominic, and Angel for everything they have done for me over the years. Your friendship and support have been truly valuable to me. Thank you all for your help and encouragement. This would not have been possible without you.

ACKNOWLEDGMENTS

I would like to express my gratitude first to Dr. Javier Macossay-Torres for his mentorship and patience these last few years as my graduate academic advisor and thesis committee chair. I would like to thank him for kindly accepting me to join his research group and helping to develop my knowledge and interest in polymer science. I wish to thank the members of my thesis committee, Dr. Hassan Ahmad and Dr. “Deb” Bandyopadhyay, for all of their assistance and guidance not only as members of my thesis committee, but also from the beginning of my undergraduate education at UTRGV to the end of my graduate program. I also wish to acknowledge Dr. Tülay Ateşin, and Dr. Abdurrahman Ateşin for motivating me to study chemistry in the first place and for the guidance they provided during my undergraduate research work. I also want to thank my fellow colleagues from Dr. Macossay’s research group, Fatema and Kingsley, who offered perspective and assistance to my project which proved to be incredibly valuable. Finally, I would like the University of Texas Rio Grande Valley and the entire of the Chemistry Department for providing such a valuable experience. The support and direction that I received from you all has proven to be invaluable and will undoubtedly serve me well in the years to come.

TABLE OF CONTENTS

Page

LIST OF TABLES

Page

LIST OF FIGURES

Page

CHAPTER I

INTRODUCTION

As the field of tissue engineering evolves, there is an increasing demand for polymer materials with properties similar to naturally occurring tissue. Such properties include biodegradability and excellent tensile strength, while ease of polymer production allows for more efficient creation of effective medical tools. Up to this point, materials scientists have looked toward different polymers, naturally derived and synthetic, to suit biomedical needs (Pham 2006). One aspect of tissue engineering that has driven the need for biomimetic materials is knee arthroplasty utilizing ligament prosthesis. Knee injuries, specifically those resulting from tearing of the anterior cruciate ligament (ACL) are one of the most common repetitive injuries in the United States, with an incidence of 100,000 cases in the US in 2010 (Cimino 2010). Annually, such injuries represent a total treatment cost of approximately 0.5 to 3 billion dollars (Spindler 2008). The major factor contributing to this insistent problem is the rejection of typical prosthesis materials such as polytetrafluoroethylene (PTFE) or polyethylene terephthalate (PET) as a response of the immune system. Typical materials face untimely degradation by the hostile synovial fluid in the knee. The synovial fluid in the knee is hostile toward foreign material to the point that even newly generated connective tissue cannot grow to repair injury without a tissue scaffold (Palmer 2011), thus a material that can serve as a functional tissue scaffold for developing cells with favorable resistance to biodegradation is necessary. In addition, the ACL is a major ligament in the knee that is primarily responsible for stabilization in knee movement.

Comprised of an anteromedial and a posteromedial bundle, the ACL also prevents hyperextension of the knee and controls rotary motion at the knee. This range of motion necessitates a material with good physical properties with respect to extension and stress capacity (Peeler 2017). Typically, ACL arthroplasty is done by surgically replacing the torn portion of the ligament with either an autograft or allograft material at anchor points along the tibial plateau (DiFelice 2015). However, due to the amount of ACL injuries, degree of degradability of donor materials, and lack of ready source of donor tissue for grafting, the potential of synthetic polymer materials is being explored. In this study, polycaprolactone (PCL) was chosen to fill this role as it has been described to exhibit good resistance to degradation (Diaz-Gomez 2014), excellent physical properties (Sayyer 2013), and because it can be processed into tissue scaffolds that have potential for anterior cruciate ligament prosthesis.

Polycaprolactone

Polycaprolactone is a polyester that has commonly been a subject of attention in medical research due to its biodegradability, physical capabilities, and practicality (Sheng 2019). PCL is nontoxic and biocompatible, allowing for cell proliferation in vivo while also maintaining excellent chemical properties such as its hydrophobicity, low melting point (60°C) and glass transition temperature (-60°C) and elastic physical nature. PCL is semicrystalline and linear in structure. It can be synthesized via the ring-opening polymerization of ε-caprolactone using a stannous octoate catalyst. Its structure is marked by the repeating ester group along the polymer chain that affords the polymer a degree of hydrophilicity. This feature does not overcome the aliphatic hydrocarbon chain that makes PCL resistant to water degradation but does allow for interaction between PCL and other substances in certain conditions.

Previously, other polymers such as polyglycolic acid (PGA) and polylactic acid (PLA) have been explored as potential polymers suitable for tissue scaffold engineering due to the biocompatibility, tailorable degradation rate, and modifiable surface properties inherent to the materials (Gentile 2014). However, this study focuses on polycaprolactone due to the superior physical properties offered by the polyester. When comparing the chemical structures of these three biomimetic polymers (Figure 1), the distinct long methylene chain of PCL offers a greater degree of elongation to the polymer, imbuing any fabricated PCL scaffolds with greater resistance to strain deformation.

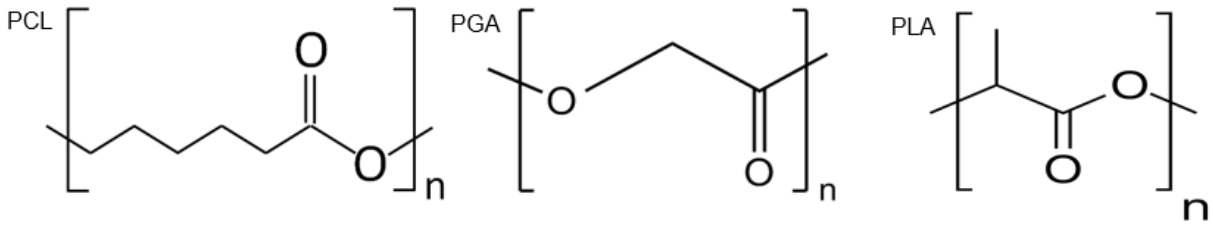

Figure 1: Chemical structures of polyesters polycaprolactone (PCL), polyglycolide (PGA), polylactic acid (PLA)

Comparing the tensile elongation at break percentages for the three polymers shows a distinct difference in their ability to withstand bending before complete loss of structural stability. When force is applied along a polymer fiber axis, this external stress changes the equilibrium interatomic distances of the polymer, thus eliciting an elastic response. PCL microfiber scaffolds are preferably fabricated with fiber alignment in mind, so as the external stress is applied along the axis of fiber alignment, there is elongation in the direction of the applied force. As this elongation occurs, the polymer chains are aligned thus strengthening the resistance of the material against complete and irreversible deformation. Thus, lengthier polymer

chains such as those of PCL are capable of more alignment under strain compared to chemicals with shorter structures or unaligned polymer samples (Khokhlov 2009). As PCL maintains an elongation at break percentage several times higher than the other polymers (Table 1), it was determined to be more suitable to meet the mechanical and structural demands presented by ACL prosthesis.

Table 1: Elongation at break percentages for biocompatible polyesters. (SpecialChem)

Material	Elongation at Break (%)
PCL	600-900%
PGA	15-20%
PLA	5-7%

There are other characteristics of PCL contributing to the attractiveness of the material for bioengineering applications such as tissue prosthesis. The most prevalent of such characteristics is the biodegradability of the polymer. Predictable and tunable biodegradability is an attractive feature for arthroplasty as it ensures that a PCL ligament prosthetic will not require surgical removal once native cells proliferate in the knee. The potential tendency of PCL to degrade from these enzymes can be attributed to the natural hydrolysis of ester bonds which is autocatalyzed by the carbonyl end groups on the polymer chain. This ester bond hydrolysis is further affected by the length of the polymer chain, the crystallinity of the sample, and the hydrophobicity of the polymer. The acute effects of biodegradation are not immediately seen in PCL studies. Typically, after 2 years in a hostile enzyme environment, a PCL allograft or autograft undergoes gradual decay until its complete dissolution (Spindler 2008). It is this observation that demands an investigation into the effect of this enzymatic environment on synthetic tissue scaffolds. The long-term effects of this metabolism are not completely known at

this point; though to avoid toxic by-products, some studies have posited the application of a copolymer to aid in maintaining elastic properties over long term degradation without adding more potentially hazardous by-products (Kanjwal 2011). The degree of degradation from other enzyme sources found in vivo such as elastases are one focus of this study.

Gelatin

To amend any issues potentially caused by the tendency of PCL to degrade over time and to improve the other properties of the compound, this study also investigates the effect of the addition of gelatin as a copolymer. PCL inherently has a high degree of miscibility, making it attractive for blending with other material that can supplement its shortcomings. In this case, gelatin was chosen as it could provide better elasticity to the tissue scaffold prototype as well as providing hydrophilic character to the prototype, making it more suitable for biomedical applications. Gelatin is a protein and a natural polymer derived from the hydrolytic degradation of collagen that contains bioactive polypeptides. As it is composed of various amino acids, gelatin has numerous polar functional groups that make it exceptionally hydrophilic and compatible to biological environments. In terms of physical characteristics, gelatin has been recorded to maintain Young's Modulus values of 414 $\pm$ 50 MPa and break-point stress 11.7 $\pm$ 1.52 MPa. This elastic character of gelatin could be advantageous for use in tissue engineering. This in combination with the nontoxic character of gelatin results in a biocompatible polymer that has the potential to improve all the shortcomings of PCL.

Anterior Cruciate Ligament

The knee joint is comprised of several ligaments and menisci that allow for the wide range of motion while protecting against knee overextension and injury. The ligament of interest

to this study is the anterior cruciate ligament so named because this tissue runs across its paired ligament, the posterior cruciate ligament. These ligaments cross over each other within the joint capsule and remain outside the synovial cavity. The ACL arises from the anterior intercondylar area of the tibia behind the attachment point of the medial meniscus and extends proximally to the posterior part of the lateral femoral condyle. As it extends across the knee joint, the ACL passes beneath the transverse ligament and blends with the anterior meniscus (Girgis 1975). The primary role of the ACL is the prevent displacement and rolling of the femoral condyles during knee flexion and to prevent hyperextension of the knee. However, ACL injuries are one of the most common knee injuries in the United States (Cimino 2010), commonly resulting from sudden stops or changes in direction causing a partial or complete tear of the tissue body.

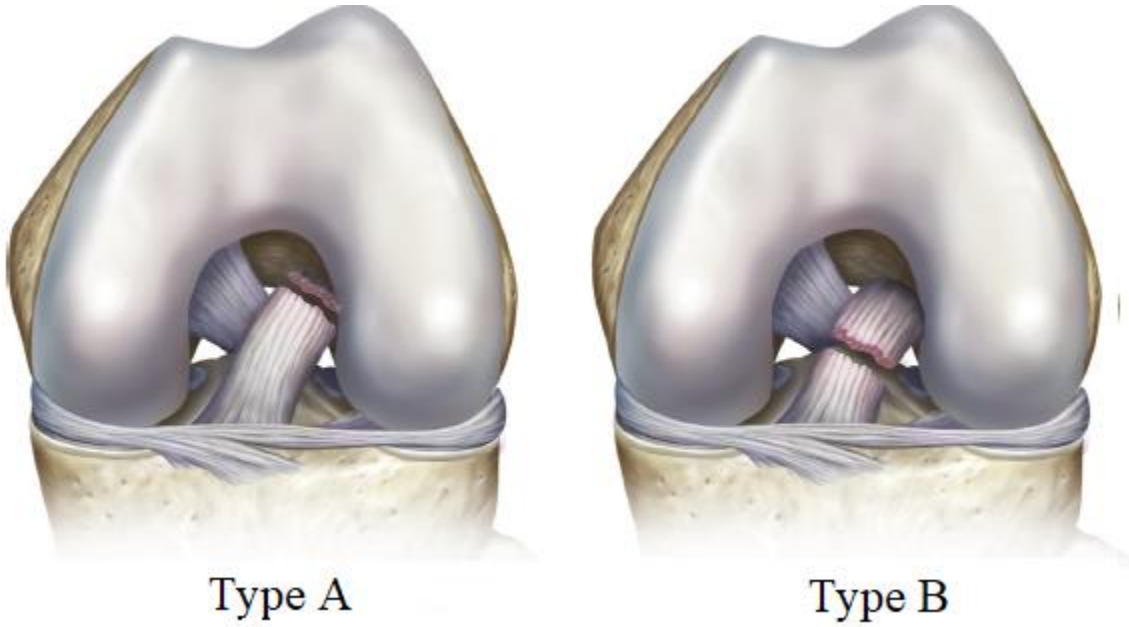

Figure 2: Different categories of ACL tear Type A (left) and Type B (right) (modified from DiFelice 2015)

The different types of ACL tear that are commonly observed (Fig. 2) present unique challenges for ligament prosthesis. In significantly older studies, patients with very little remaining connective tissue left on the femur (Type A) were the only patient group with realistic opportunity for tissue repair as previous surgical procedures relied on directly suturing the remaining ligament tissue to the ACL "stump" and allowing for natural tissue regeneration to occur. It was concluded that the direct attachment of the torn ligament to the femoral origin and higher quality of tissue was responsible for better patient recovery (Sherman 1991), leaving many patients with mid-substance tears (Type B) without treatment options. This is one advantage of developing polymer tissue scaffold prosthetic prototypes for use in ACL repair. Through the utilization of completely fabricated polymer microfiber scaffolds, there is potential to "bridge" torn ligament tissue offering the structural support previously unavailable to Type B patients. Such scaffolds also can allow for the proliferation of new tissue cells with the loss of ligament strength inherent to sutured ACL tissue. More contemporary studies have found that older ACL restoration studies were unable to determine other variables that affected patient recovery rate such as the degradation effect of the synovial fluid enzyme environment on repaired ACL tissue (DiFelice 2015)

Once torn, the ACL is easily reinjured due to the harsh synovial environment of the knee (Palmer 2011). Synovial joints contain a healthy volume of synovial fluid to provide lubrication for articular cartilage and facilitate movement, absorb shock to the joint, and transport and filter nutrients and waste. This non-Newtonian fluid is comprised of primarily hyaluronic acid and a variety of proteinases and collagenases (Lee 1996) that pose a significant problem for arthroplasty. Upon injury of the ACL, an inflammatory response is triggered, and the knee joint is flooded with synovial fluid (Tchetverikov 2005). Over time, the sustained release of this

synovial fluid can potentially degrade newly generated tissue and make neoligamentization impossible. Thus, exploring the resistance of electrospun tissue scaffolds is vital to the feasibility of future prototypes. Although previous studies have utilized hydrophobic and degradation-resistant materials such as polyurethane (Liljensten 2002)(Macossay 2014) over time, the enzymatic environment of the synovial joint proves too hostile for cell proliferation and blood vessel growth in the new ligament. A suitable tissue scaffold prototype would need to be able to resist such an environment while maintaining biocompatibility for tissue growth and regeneration of the ACL.

As knee ligament arthroplasty is a major goal for this study, being able to design a tissue scaffold with the dimensions of the ACL is of high priority. Previous studies have recorded average dimensions of the ACL as presented in Table 2.

Table 2: Anterior Cruciate Ligament Length, Width, Thickness

Anterior Cruciate Ligament Dimensions			
	Average Measurement	Range	Std. Dev.
Width **n=66**	8.23 mm	5.1 – 13.7 mm	1.96
Length **n=66**	32.4 mm	22.9 – 45.1 mm	4.06
Thickness **(Sagittal Plane)** **n=48**	4.5 mm	3.1 – 7.2 mm	0.9
Thickness **(Frontal Plane)** **n=48**	4.3 mm	2.9 – 6.2 mm	0.8

Because factors such as nutrition and genetics have a major effect on human growth and development, the dimensions of body parts including knee ligaments vary from population to population over different periods of time. This results in difficulty generating a one-size-fits-all approach to creating knee ligament prosthetics for individual patients. This issue has been

investigated by numerous research groups who have identified statistically significant correlations between easily measurable physical attributes such as height or femoral width and ACL length (van Zyl 2016) to allow for accurate predictions of ligament dimensions and thus medically applicable tissue scaffold prototypes. Nevertheless, the average ACL dimensions such as length, width, and thickness (de Oliveira 2015) for some populations have been documented in the course such studies. These average ACL dimensions can act as broad goals for the dimensions of a fabricated PCL microfiber tissue scaffold prototype.

Ring-Opening Polymerization

In this study, polycaprolactone synthesis is achieved through ring-opening polymerization (ROP) of ε-caprolactone (ε-CL) in the presence of a catalyst. ε-CL is a cyclic monomer containing a polar carbonyl group which lends itself well to the ROP process, yielding a high molecular weight, low dispersity polymer. While it is more expensive than other methods of PCL synthesis such as polycondensation, ROP produces a high-quality PCL that is suitable for the needs of this study.

The catalyst utilized in the ROP reaction for this study is tin (II) 2-ethylhexanoate, commonly known as stannous octoate [$Sn(Oct)_2$]. Approved by the FDA as a food additive, $Sn(Oct)_2$ is an inexpensive and versatile catalyst that is easily applicable to this study due to its solubility in organic solvents and lactones. Although FDA approved, $Sn(Oct)_2$ is composed of a toxic metal that can potentially be present in the synthesized polymer. Even in trace amounts, tin can form cytotoxic compounds making its use in the synthesis of PCL for tissue engineering pursuits less attractive. There have been investigations into the use of other, less toxic metals such as magnesium and calcium alkoxides as catalysts to supplant $Sn(Oct)_2$ in these types of ROP reactions (Kricheldorf 2007).

The mechanism that ring-opening polymerization of ε-caprolactone follows is a topic of ongoing study. Previous investigation (Obregon 2018) asserts that two primary mechanisms are the most probable: the activated monomer type and the monomer-insertion type. In activated monomer polymerization, direct coordination of the stannous octoate catalyst with the carbonyl oxygen of ε-caprolactone activates the monomer (Fig. 3).

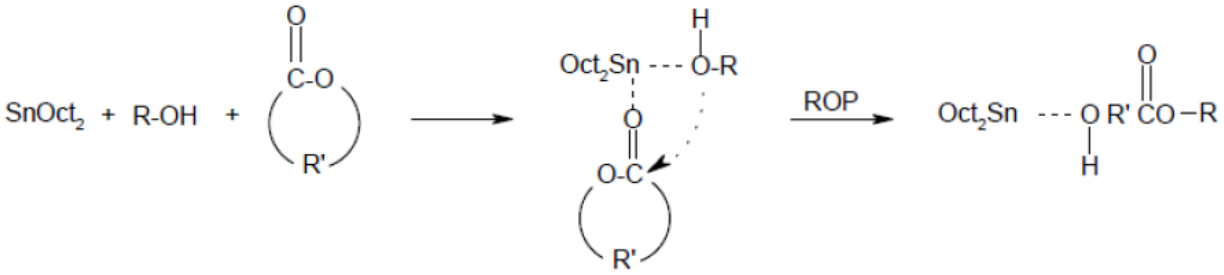

Figure 3: Activated Monomer Mechanism for ROP of Lactones (Obregon 2018)

This activation makes the carbonyl oxygen of the monomer more susceptible to nucleophilic attack, leading to further reaction with an alcohol (either as an impurity or added intentionally). After the nucleophilic attack of alcohol, a rearrangement of electrons occurs, allowing for the insertion of the monomer into the metal-oxygen bond. Propagation of the polymerization continues as both monomer and alcohol are coordinated to the $Sn(Oct)_2$ complex until a hydroxyl group formed during hydrolysis terminates the reaction (Albertsson 2003).

In monomer-insertion type ROP, Sn(Oct)2 is suggested to act as a co-initiator in the presence of alcohol (Penczek 1998). In this proposed mechanism, alcohol reacts with Sn(Oct)2 producing a stannous alkoxide active specie with a free 2-ethylhexanoic acid before polymerization begins (Fig. 4).

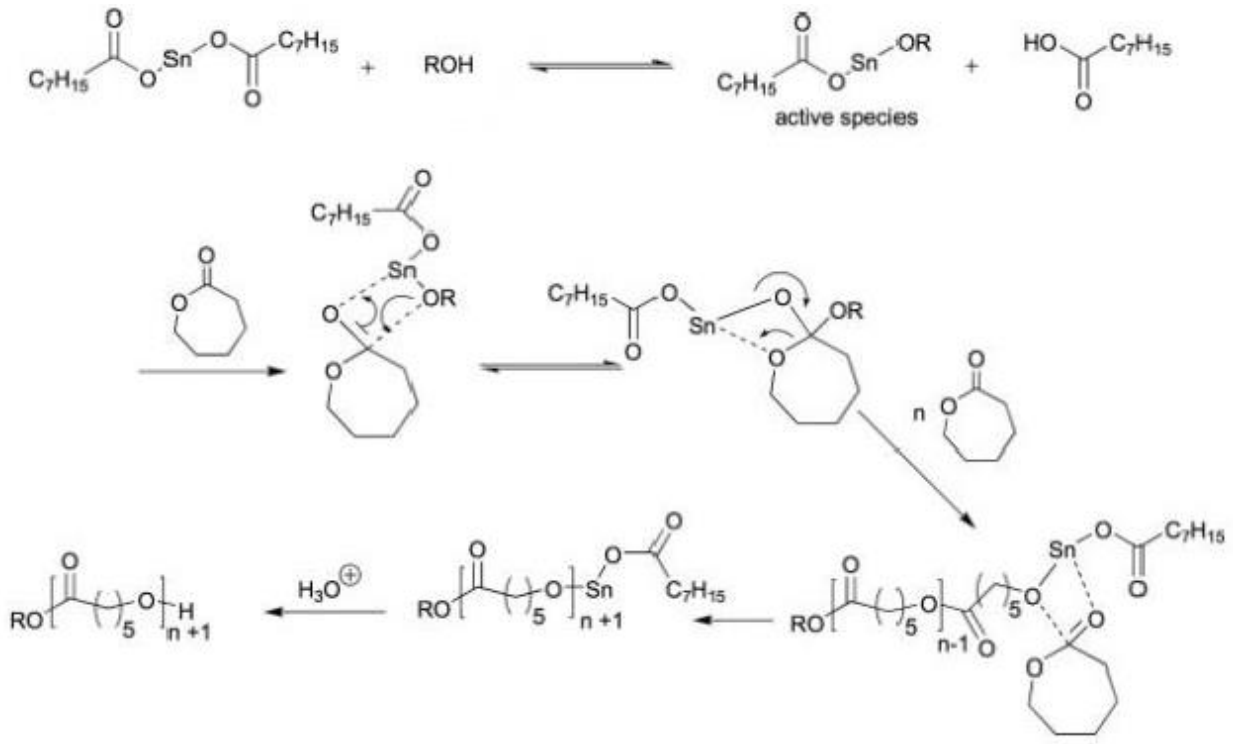

Figure 4: Monomer-Insertion Mechanism for ROP of ε-CL (Obregon 2018)

This stannous alkoxide acts as the initiator of the polymerization, coordinating to the carbonyl of the monomer to begin the ring-opening step of the reaction. The now nucleophilic alkoxide is added onto the electrophilic ester functional group of ε-caprolactone. The reaction then proceeds via acyl-oxygen bond cleavage, opening the ring and forming a new alkoxide which acts as the propagation center. The propagating polymer chain remains attached to the metal via the alkoxide bond until a hydroxyl end-group formed by hydrolysis terminates the reaction.

To achieve a higher degree of reproducibility, scalability, and cost-efficiency, microwave irradiation is employed as an alternative energy source to improve the outcome of the ROP reaction. Microwave irradiation heats molecules via molecular dipole moments being impacted by microwave energy. Any molecules that exhibit permanent dipole moments will undergo

rotation, friction, and collision resulting from their alignment to the applied microwave electromagnetic field, thus generating heat (Hoogenboom 2007). ε-CL consists of a polar carbonyl group with a loss tangent (tan δ: the ability to translate electromagnetic energy into heat at a given frequency and temperature) of 0.35. Being that tan δ values 0.1 to 0.5 indicate moderation absorption of microwave radiation, microwave assisted ROP of ε-CL was determined to be a fast and high-yield method for synthesizing high molecular weight PCL.

Electrospinning

Electrospinning is a process that originates from the mid-20th century as a novel method of spinning fibers for filtration tool manufacturing from biopolymers such as cellulose acetate based on even earlier efforts to refine electrospraying procedure (Filatov 2007). However, in the mid-1990s, polymer scientists such as Reneker demonstrated the applicability of organic polymers to the electrospinning process (Reneker 1995), near-instantly popularizing the technique and vastly increasing the field of work for electrospinning and solidifying it as a multifaceted and tremendously applicable tool for micro/nanofiber engineering. In the present, electrospinning is a robust tool for polymer fiber fabrication with highly tunable experimental parameters that result in fiber scaffolds suitable for various projects. Electrospinning is the chosen method of fabrication for the PCL microfiber tissue scaffolds in this study as it has been established to allowed good control of the physical characteristics and porosity of the completed fiber mats (Pauly 2019), both attractive aspects for tissue engineering. As pictured in Fig. 5, electrospinning involves ejecting a polymer solution from a electrically charged spinneret (typically a metal needle) onto target charged with equal but opposite charge. Utilizing the generated electric field, this technique can provide fiber samples with 10 nm to 10 μm diameter features (Cramariuc 2013).

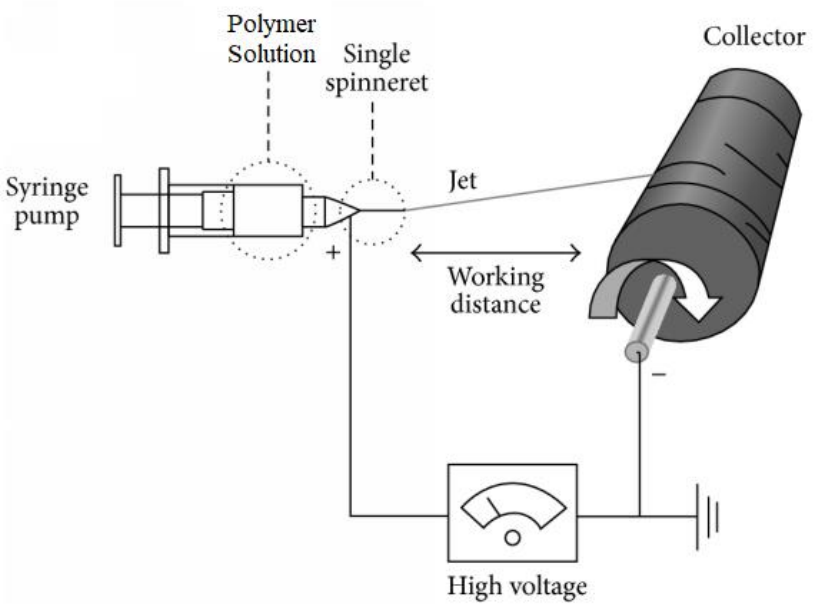

Figure 5: Schematic diagram of a typical electrospinning setup with rotating collection drum (Mori 2015)

By applying sufficient charge to a polymer solution, electrostatic forces overcome surface tension and droplets are stretched, eventually ejecting a stream of polymer solution from a point of eruption known as a Taylor cone. As the stream moves toward the oppositely charged collector, it dries and gains acceleration before deposition. This acceleration results in elongation which leads to uniform fibers at diameters as small as the nanometer scale. By utilizing a rotating collector drum, the deposited fibers can be aligned along the direction of rotation, improving elongation of the microfiber mats thus affecting the tensile properties of the completed fiber scaffold. The parameters of an electrospinning setup such as electric potential, flow rate, solution viscosity, and needle characteristics are carefully chosen as they directly influence the qualities of the finished microfiber mat. For example, voltage settings can improve fiber diameters by stretching polymer solution as it is jetted, though excessively high voltage can destabilize the jet

resulting in the opposite effect. In addition, high solution viscosity can prevent ejection from the jet, leading to discontinuous fiber formation and beading of deposited polymer on the sample surface (Ginestra 2016). Being that electrospinning parameters have a major influence on the physical characteristics of a fabricated polymer mat, high priority properties such as fiber alignment and surface porosity are controlled to ensure a suitable prototype can be fabricated.

Enzyme Degradation

To ensure that the PCL tissue scaffolds are suitable for the hydrolytic environment of the knee, this study simulates a synovial environment on the higher end of enzyme concentration as described in the methodology section. Generally, polyesters are more susceptible to hydrolytic degradation proportionally to their hydrophilic character. Thus, PCL is better suited for environments compared to PGA or PLA (Jeong 2004). Synovial enzymes are hypothesized to collectively affect the healing of intra-articular injuries (Maeda 1995), which makes it a critical matter to determine how new materials will fare in their presence. Synovial fluid is primarily composed of D-N-acetylglucosamine and hyaluronic acid as well as lubricin glycoproteins and various enzymes such as proteinase, collagenase, and elastase (Seidman 2021). Of these enzymes. elastase and matrix metallopeptidase 1 (MMP-1) are found in varying concentrations. Elastase is a class of protease that primarily targets and breaks down elastin and collagen fibers which, in combination, control the mechanical properties of various connective tissues. In the knee, the specific protease present is neutrophil elastase which destroys bacteria and host tissue alike via hydrolysis. In this process the proteins are degraded in specialized neutrophil lysosomes which further degrade other proteins in the extracellular matrix. MMP-1 is a collagenase that specifically targets Types I, II, and III interstitial collagen for degradation. It is also known to be involved in the breakdown of the extracellular matrix and tissue remodeling. Typical bodily

concentrations of these enzymes can range. Elastase concentration in the knee can range from 0.041 to 101.8 µg/mL. MMP-1 concentration can range from 177 to 279 µg/mL in the knee (Palmer 2011).

CHAPTER II

METHODOLOGY

Starting Materials

ε -caprolactone was purchased from Acros Organics. Stannous octoate [$Sn(Oct)_2$] was purchased from Silicone Technology and stored under refrigeration. 100% beef gelatin was sourced from PB Leiner. The solvents dichloromethane (99.8% extra dry), dimethylformamide (≥99.9%) and tetrahydrofuran (≥99.8%) were purchased from Acros Organics. Hexane (99.9%) was purchased from Sigma-Aldrich and stored under freezing conditions. All chemicals were used without any further purification. For the biodegradation trials, the MMP-1 (295 u/mg dry weight) and elastase (11.5 u/mgP) were sourced from Worthington Biochemical.

Microwave-Assisted Ring-Opening Polymerization

The Anton Paar Monowave 400 was used to carry out the microwave-assisted reaction. The reaction temperature was set to 150°C for the complete duration of the polymerization. This temperature was maintained via the internal IR laser thermometer in the instrument. The reaction proceeded for two hours at peak temperature, followed by one hour of cool down to room temperature. The maximum pressure in the reaction chamber was set to a 5.5 torr. A mixture of 3.42 g of ε-caprolactone (30 mmol) and 10.7 µL of stannous octoate catalyst (0.0033 mol) was poured into a microwave reaction flask with a magnetic stirring bar. The reaction flask used was the 30 mL Anton Paar G30 borosilicate model, a vessel designed specifically for the 400 series

Monowave with a maximum fill volume of 20 mL. The flask was purged with Argon gas for 10 minutes, sealed, and transferred to the microwave reactor. The vessel was irradiated at reaction conditions before being removed from the monowave reaction chamber and allowed to cool and solidify.

Polymer Extraction

Upon completion of the reaction, the solid product was dissolved in 6.0 mL of dichloromethane and the contents were poured into a precipitation dish or large beaker. The dissolved PCL was then precipitated with 15 mL of cold hexane and the dish was moved to the freezer for at least 24 hours. After this, the precipitated PCL was gently vacuum filtered and moved into 20 mL scintillation flasks to be dried and stored in a Isotemp Model 280A vacuum oven at 45°C under 25 in. Hg.

Fourier Transform Infrared (FTIR) Spectroscopy

Infrared spectroscopy characterization was carried out using a Bruker VERTEX 70v FT-IR spectrometer equipped with a diamond crystal tip. The instrument in conjunction with OPUS software completed scans with resolution set to 2 cm^{-1}, 256 scans and a frequency range of 3500 cm^{-1} to 400 cm^{-1}. PCL samples were crushed into fine powder and loaded onto the spectrometer analysis platform for characterization.

Scanning Electron Microscopy

To determine the degree of gelatin adherence achieved during the coating step, scanning electron microscopy was employed to obtain images at 5000X and 20,000X magnification. The instruments used were a Zeiss LEO 435 VP scanning electron microscope with a Denton Vacuum Desk II self-contained sputter and etch unit. To achieve imaging, the microfiber

samples were treated with an ultrathin coating of palladium (Pd) through low vacuum sputter coating. This electrically conductive alloy coating prevents static electric charge during electron irradiation thus improving the signal and enhancing image contrast and resolution. During Pd coating, the argon pressure in the vacuum chamber was set to 6-7 psi. The samples were loaded onto a pedestal holder and sputter deposition was initiated when the chamber reached 30 mTorr or below. The samples were coated in two consecutive 30 second cycles at 45 mA. Upon completion of coating deposition, the samples were placed on a silicon wafer and moved into a sample chamber wherein micrographs were taken at various magnifications. Micrographs were obtained from the microscope operating at an accelerating voltage of 3.9 kV and set aside for comparison.

Electrospinning

Electrospinning was carried out with a custom rotating mandrel machine at atmospheric conditions and at room temperature. An Extech Instruments 382213 DC regulated power supply was used to supply the voltage potential to the spinneret and collection drum. The electrospinning parameters were decided based on previous work carried out with microwave assisted ROP derived PCL (Obregon 2018). The positive voltage for the system was set to +12kV and the negative was set to -12kV. The positive voltage was transferred from the power supply to an alligator clip connected to a 21-gauge blunt-tipped needle spinneret. The negative end was grounded to the collector apparatus which was a cylindrical section of machined stainless steel 10 cm in diameter, rotating at a constant rate of 2500 rpm to promote fiber uniformity and alignment. Here, the positive character on the spinneret induced an attraction between the now positively charged polymer solution and the negatively charged collector disk. The polymer solution consisted of 8 mL of a 15% wt/vol PCL solution in 1:1 (DMF:THF)

dispensed from a 10 mL glass syringe. The contents were administered for electrospinning by a KD Scientific 200 syringe infusion pump programmed at a flow rate of 0.2 mL/min.

Gelatin Coating

The completed fiber mats were coated with gelatin to investigate the effect of the natural polymer on the physical properties of PCL. To coat the fiber mats, a 5% wt/vol beef gelatin solution was prepared using a 1:1 ratio of hot water (~95 C) to acetic acid. The solution was poured into a 20 mL scintillation flask and stirred overnight to dissolve the gelatin powder. Once fully dissolved, the gelatin solution was poured into a petri dish containing sections of a PCL fiber mat. The petri dish was then placed into a desiccator with all the calcium chloride removed and replaced with another petri dish filled with water. This was done to ensure the environment remained hydrated for the duration of the coating. The samples were left in the desiccator for at least 24 hours and removed when needed for further testing.

Tensile Strength Testing

The tensile testing of the PCL and PCL+Gel fiber samples was carried out using an INSTRON tensile tester 5943 with a 25 N maximum load cell under a crosshead speed set to 10 mm/min. Samples designated for testing were cut into a “dog-bone” shape using a custom-made die and lever-operated press. The dog-bone samples measured a 2.75 mm width at their narrowest point with a gauge length of 7.5 mm. A Fischer Scientific digital caliper was used to measure the thickness of each cut sample. A minimum of seven samples were used to test the tensile behavior of the polymer samples and the average values were recorded.

Tensile testing was also performed on samples after braiding with a commercial-grade hair braider. The braiding instrument was a Hanmei™ Twist Secret hair braider obtained from an online retailer.

Enzyme Degradation Study

To measure and compare the tendency toward degradation of the PCL and PCL+Gel fiber samples, a simulated synovial fluid formulation was prepared. To emulate the hostile conditions of the knee, enzyme solutions were prepared at the higher end of physiological concentration ranges. The enzymes utilized for this study were MMP-1 (250 µg/mL) and elastase (100 µg/mL). Stock solutions of each enzyme were prepared using phosphate buffered saline (PBS) and stored under freezing temperatures. As PBS was the carrier to deliver the enzyme in each of the degradation tests, the buffer solution was also evaluated to determine its influence on the gelatin coating and greater scaffold constitution.

The degradation study was carried out by cutting polymer samples from the larger mat with a standard-size handheld hole puncher. Cut scaffold samples measured 6 mm in diameter with an average thickness of 0.14 mm measured with digital calipers. The scaffolds were placed in 12-well plates containing the enzyme and PBS solutions and allowed to incubate. After 1, 3, and 7 days, the samples were removed from the wells and analyzed via microscopy and mass loss-measurements to determine their degree of biodegradation.

CHAPTER III

RESULTS AND DISCUSSION

Fourier Transform Infrared (FTIR) Spectroscopy

The primary characteristic peaks of PCL as seen on the experimentally determined FTIR spectrum are at 1721 cm^{-1} and 2850/2900 cm^{-1}. Literature cites characteristic peaks at 1720 cm^{-1} as carbonyl stretching from the ester group of PCL while 2800 cm^{-1} to 2900 cm^{-1} peaks are attributed to methylene C-H stretching from the long hydrocarbon polymer chain (Gorodzha 2015). The results of the FTIR characterization confirm that the ring-opening polymerization was occurred and PCL was successfully synthesized with no discernable side products.

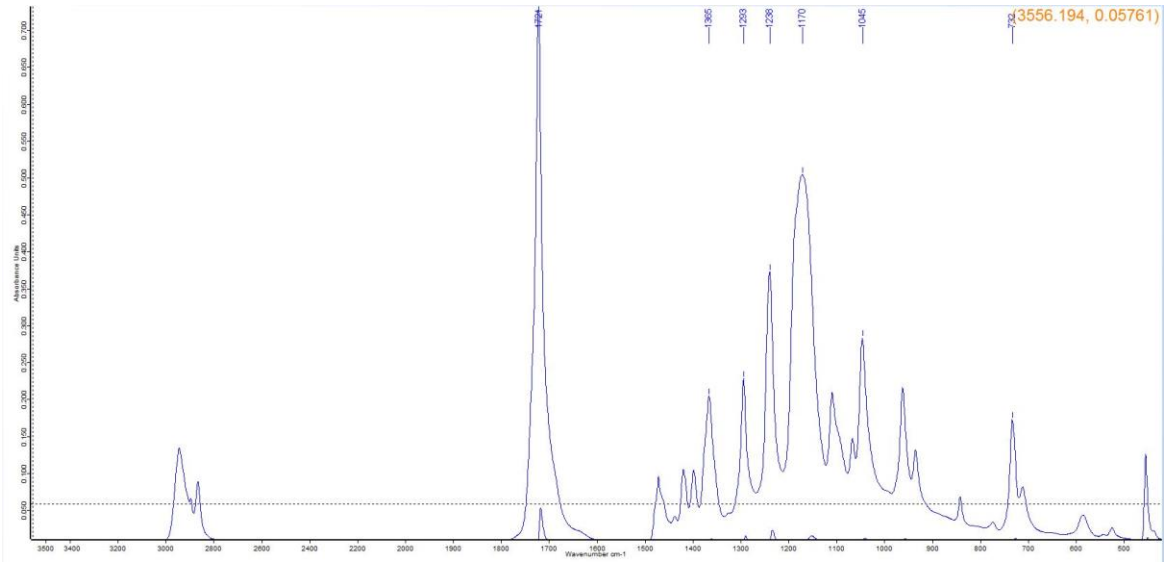

Figure 6: FTIR Spectrum of PCL

Scanning Electron Microscopy

Scanning electron microscopy yielded images that offer a better look at the surface morphology of the electrospun PCL scaffolds and the gelatin coated scaffolds. Figure 6 shows the surface character of electrospun PCL at 5,000x magnification. The uncoated PCL sample demonstrates good fiber alignment with minor beading. Overall fiber alignment tends to increase the tensile strength of the sample in resisting deformation, demonstrating the advantage of the electrospinning parameters specified in this study. Although surface beading is often observed after electrospinning (Fong 1999), further modification of the electrospinning parameters could be performed to fine-tune the surface features of the fiber mat. The uniform PCL fiber diameter also results in a high degree porosity on the sample surface as illustrated in higher magnification (Fig. 7). While high porosity is an attractive feature for biomaterials, the aligned network of fibers can also lead to small pore size, which limits cell migration into the tissue scaffold (Wright 2011).

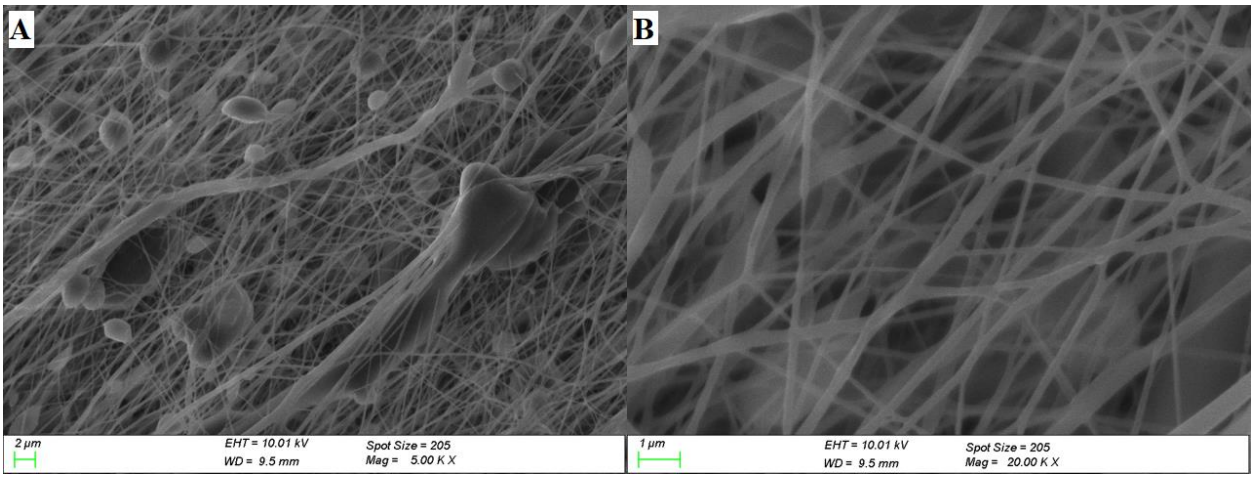

Figure 7: Scanning Electron Microscope Imaging of Aligned PCL fibers at 5,000x (A) and 20,000x magnification (B)

SEM was also carried out at the same levels of magnification for a PCL microfiber mat coated in a 5% gelatin solution. A consistent surface application of gelatin has been document to improve biocompatibility and cell viability of PCL fibers in bone implant studies (Mojarad 2019), so it was hypothesized that this process could also be beneficial for ligament tissue engineering. Fig 8A demonstrates that adequate gelatin coating was achieved across the surface of the polymer sample. Here, one can see that surface porosity of the PCL mat was maintained which, in conjunction with the hydrophilicity and biocompatibility inherent to gelatin, should improve the chances of cell proliferation on and inside the fiber scaffold.

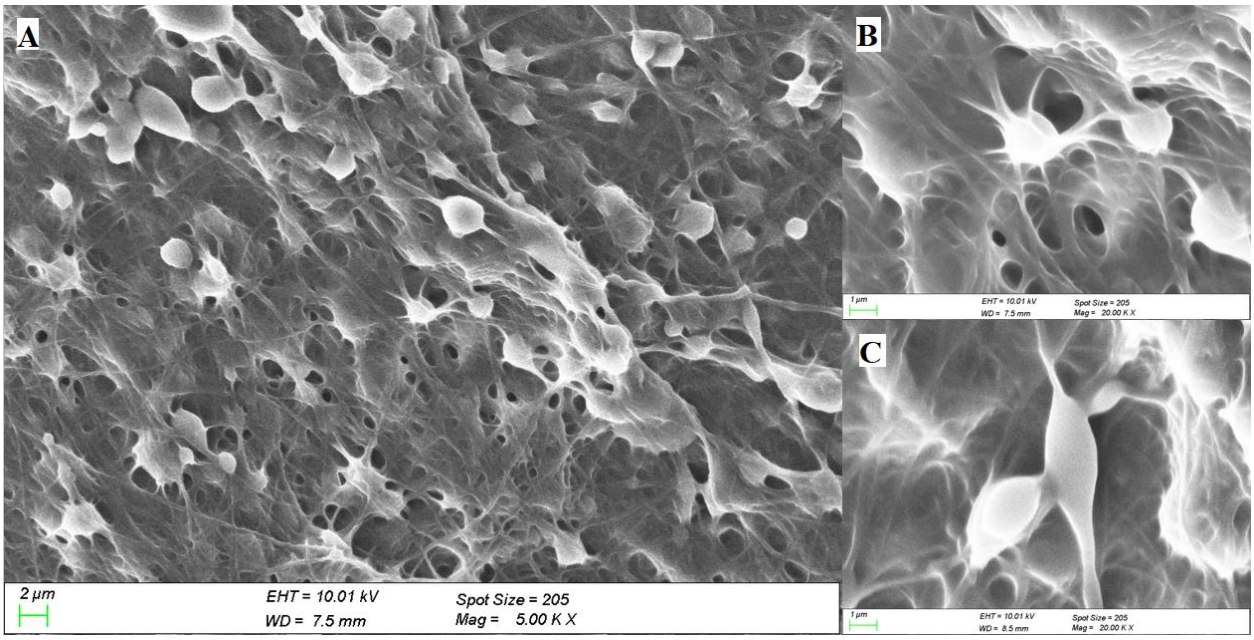

Figure 8: Scanning Electron Microscope Imaging of Gelatin-Coated Aligned PCL fibers at 5,000x (A) and 20,000x magnification (B)(C)

Figures 8B and 8C show the coating of gelatin upon the microfiber beads at higher magnification, offering a more detailed look into the minute surface features of the fiber sample. Here, one can see that the gelatin coating appears to be more heavily deposited at sections of microfiber with more beading. To amend this issue and potentially increase the effect of gelatin

on the properties of the fiber scaffold, further work could be done to include gelatin in the polymer solution during electrospinning. While is outside the current breadth of work of this study, other polymers investigations suggest the potential of such an idea (Feng 2012).

Tensile Strength Testing

Tensile testing was carried out for three distinct electrospun PCL fiber scaffolds to determine their physical properties. The first group of samples were taken from a PCL fiber scaffold that was fabricated with a low degree of fiber alignment. The results of tensile testing for the non-aligned fiber samples are illustrated in Figure 9.

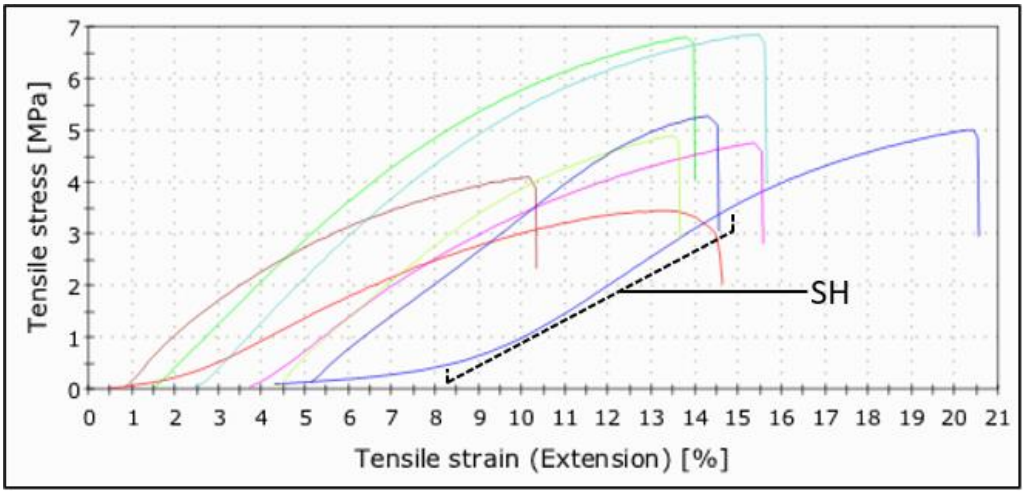

Figure 9: Tensile Strength Test of Non-aligned PCL fiber mat. All samples were taken from the same electrospun sheet.

Table 3: Non-aligned PCL fiber mat Tensile Test Results

Non-aligned PCL fibers	Max Load	Tensile Stress	Tensile Strain	Young's Modulus
Mean	5.273 N	5.143 MPa	0.120 mm/mm	73.7 MPa
Std. Deviation	1.20	1.18	0.023	18.16

Here, we can see that while some samples show decent physical properties as expected from PCL, there is an undesirable range in individual sample results. Tensile strain values ranging from 10% to 20% demonstrate a lack of consistency stemming from differences in the polymer web of each sample. As there is no fiber alignment in this trial, polymer crosslink density is increased which restricts molecule mobility resulting in brittleness. In addition, some samples exhibit an immediate plateau of the tensile curve before smoothing out for an upward slope. This is known as strain hardening (SH) and occurs as the fiber undergoes large scale orientation due to an applied force resulting in better elongation properties. This visualization of the effects of strain deformation on the tensile curve is prevalent in the non-aligned fiber samples as they begin testing without much fiber orientation. The non-aligned PCL fiber samples demonstrated good tensile strength at break values and maintained good maximum load although individual samples displayed an unfavorable degree in variance across all trials.

While the tensile results show that even non-aligned PCL fibers maintain some good physical properties, there is a need to achieve more consistent results. To that end, new samples were taken from microfiber mat scaffolds fabricated with high alignment from a thinner (0.04mm thick) section of the electrospun mat. The samples used in this testing process were cut along their fiber alignment and extended to the breakpoint to quantify and visualize their physical properties.

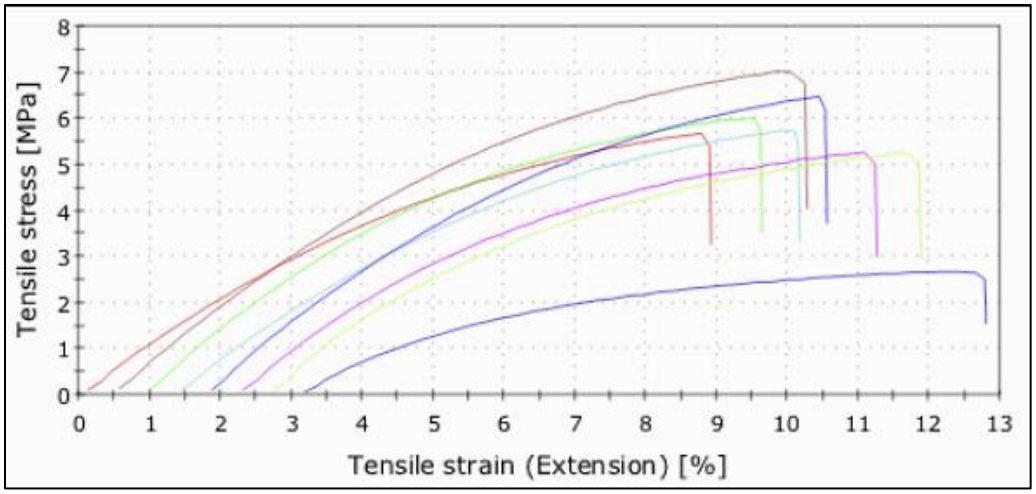

Figure 10: Tensile Strength Test of Aligned PCL fiber mat. All samples were taken from the same electrospun sheet.

Table 4: Aligned PCL fiber mat Tensile Test Results

Aligned PCL fibers	**Max Load**	**Tensile Stress**	**Tensile Strain**	**Young's Modulus**
Mean	3.278 N	5.515 MPa	0.089 mm/mm	124.7 Mpa
Std. Deviation	0.54	1.29	0.0025	17.02

The samples from this section of material show more consistency across all testing properties. Sample extension was more consistent, with tensile stress peaking at 7 MPa and averaging 11% extension. In this trial, fibers were more oriented before testing which is reflected in Figure 10. There is no evidence of strain hardening as the fibers yield point is not immediately reached, leading to consistent tensile strain values which suggests a more "hard and strong" tensile character compared to the "soft and tough" character (Morales 2010) of the non-aligned fiber trial. The aligned fibers in Trial 2 withstood a 37.8% lower maximum load compared to Trial 1. The test result that most clearly demonstrates the physical differences between the non-aligned and aligned fiber trials is the Young's Modulus. The Young's Modulus (YM) (also known as the modulus of elasticity) is a mechanical property that quantifies the relationship

between tensile stress and axial strain. YM is a measure of the stiffness of a material in response to elastic deformation. There was a 69.2% increase in the Young's Modulus values after using aligned fiber samples. This suggests that implanted PCL tissue scaffolds have the potential to resist elongation deformation allowing for good stabilization of the ligament repair site. There remains room for improvement of physical properties in all categories. To investigate methods of improving the physical characteristics of the microfiber scaffolds, aligned-fiber PCL samples were coating with beef gelatin and mechanically tested.

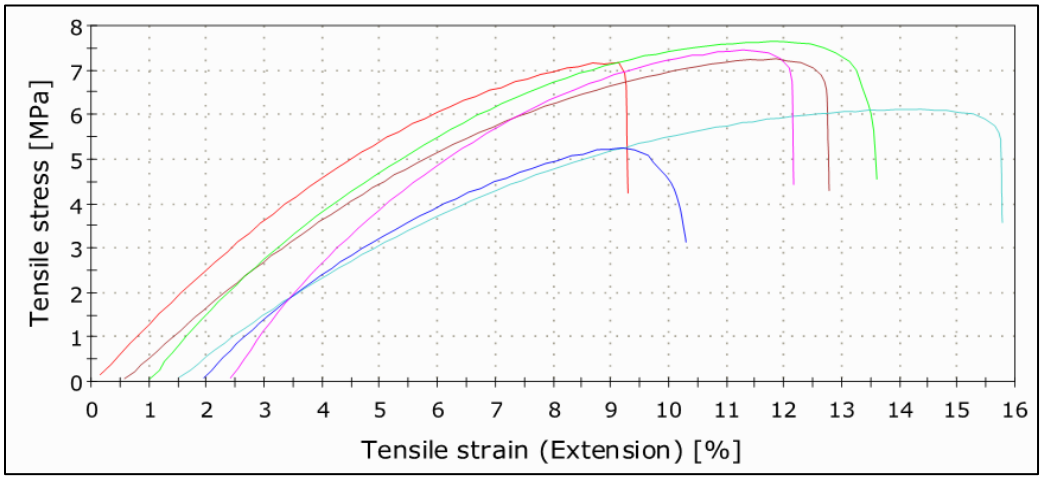

Figure 11: Tensile Strength Test of Gelatin-Coated Aligned PCL fiber mat. All samples were taken from the same electrospun sheet.

Table 5: Gelatin-Coated Aligned PCL fiber mat Tensile Test Results

Gel-coated PCL fibers	Max Load	Tensile Stress	Tensile Strain	Young's Modulus
Mean	4.874 N	6.692 MPa	0.1035 mm/mm	127.35 MPa
Std. Deviation	0.785	0.9814	0.0216	20.34

The data illustrated in Fig 11 shows that the addition of a gelatin coating improved the consistency of the tensile data for the scaffolds across the board. The addition of the gelatin

coating afforded the PCL microfiber mats improved maximum load, greater average extension, and higher YM when compared to the non-coated samples in Trial 2. Comparing the results of all three trials (Fig. 12), the gelatin-coated PCL samples are characterized by the favorable physical properties of each other trial. This is thought to be the result of a plasticizing effect imbued by the gelatin on the scaffold surface. This plasticizing effect is hypothesized to impart similar maximum load bearing strength and elongation as seen in the non-aligned fiber trial while maintaining the superior Young's modulus of the aligned fibers in Trial 2.

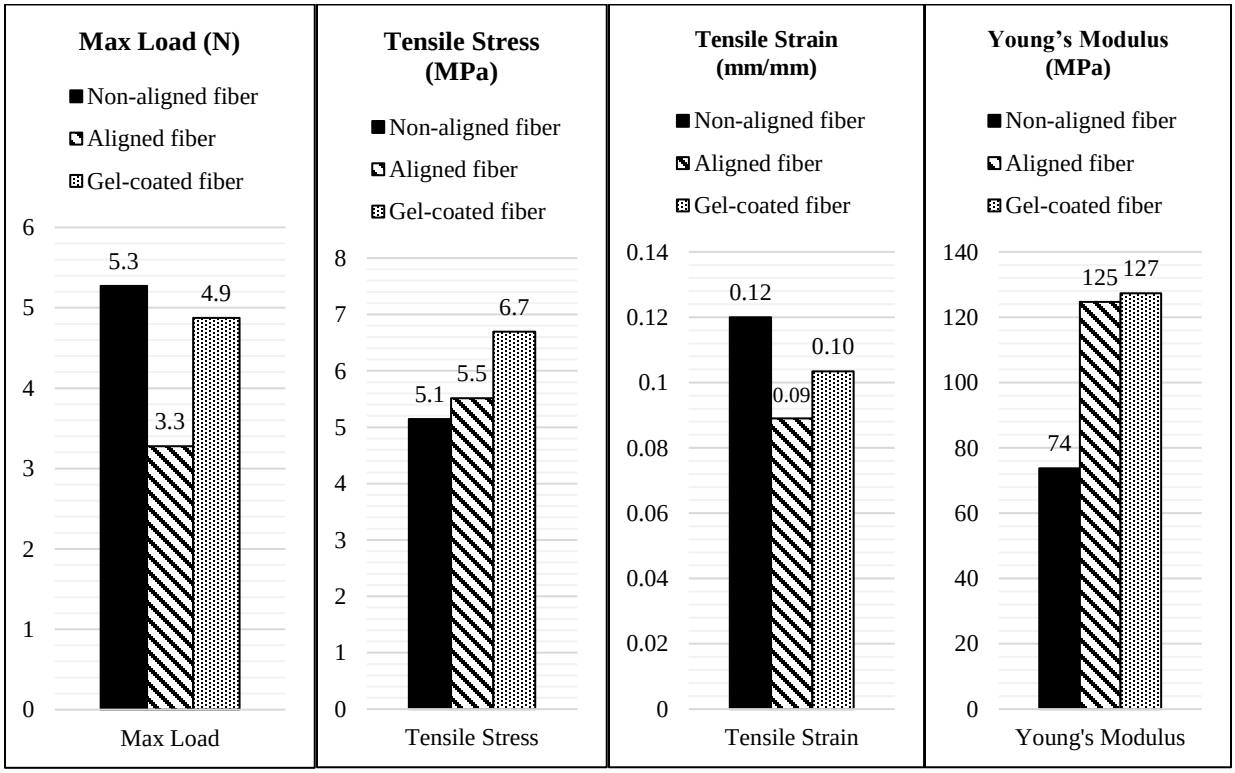

Figure 12: Comparison of Mechanical Properties for Nonaligned, Aligned, and Gelatin-Coated Aligned Fiber PCL fiber mats

Previous studies (Obregon 2018) demonstrate PCL synthesized with microwave assistance can show excellent physical properties – with extension rates of 50%, tensile strains over 10 MPa, and Young's Modulus over 50 MPa. The differences between those tensile test

results and those obtained in this study are apparent. The addition of the gelatin coating to aligned PCL fiber mats resulted in Young's Modulus measurements reaching over 100 MPa while tensile strains were measured only at approximately 10%. Overall, the effect of the gelatin coating overall is a positive one. It affords the attractive physical properties of the natural polymer. The tensile data of this test shows that the relationship between stress and strain, while consistent on their own, does not show replicability as a function. This is represented in the Young's Modulus data point. Here, it can be observed that there is still room to improve functional reproducibility either by modifying the polymer solution composition, electrospinning parameters, or gelatin coating conditions.

To provide another dimension of structural stability, it was hypothesized that braiding the PCL fiber mats could impart more tensile strength to the samples. As such a prototype would be fabricated to the ligament of an individual patient, the length and wide of a braided fiber must be comparable to that of an average anterior cruciate ligament. ACL length corresponds with the height of an individual, and thus varies widely from case to case. In addition, the length of a PCL microfiber mat can be controlled by altering the collecting drum diameter during electrospinning. For these reasons, this section of study focuses on matching only the width of the ligament. First, this process was tested using a single lab-grade paper tissue wiper. A single braided paper sample was found to have a width of 4.8 mm (Fig. 13). On average, a normal ACL has a width of approx. 8.3 mm (van Zyl 2016). One braided tissue sample only measured approximately half of the target width, so two braided samples were combined. Two braided samples measured 8.3 mm in width, indicating that a similar method would need to be undertaken with a gelatin-coated PCL fiber mat. With a target width recorded and proved reachable, coated PCL fiber mats were braided and measured.

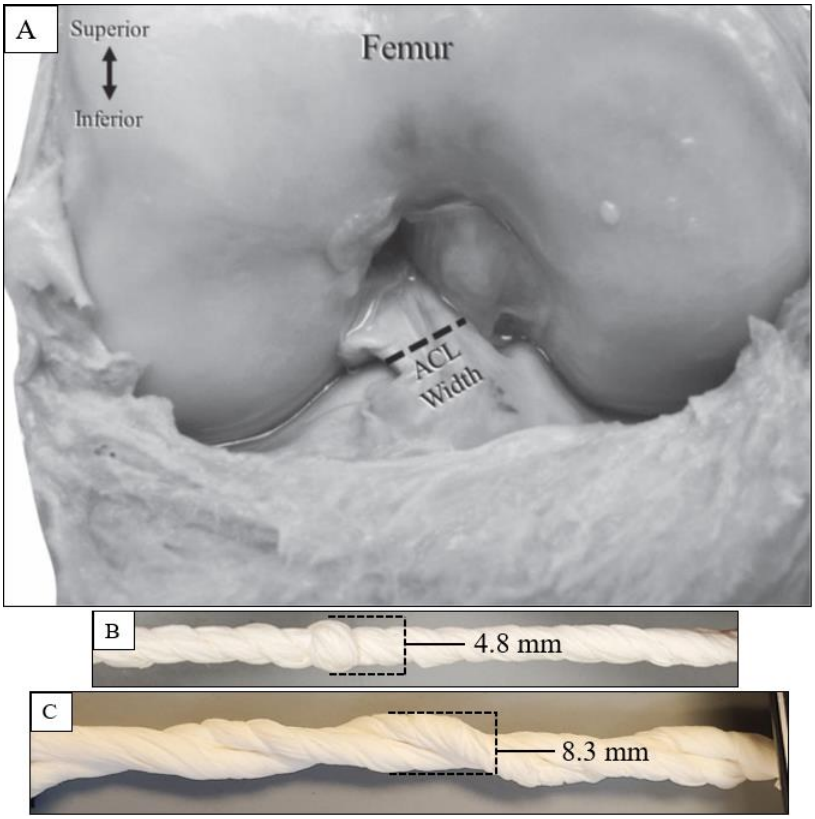

Figure 13: Section of ACL used to Determine Average Width (A), Measured Width of Single-Braided Tissue (B), Measured Width of Double-Braided Tissue (C)

During braiding, some limitations of the gelatin-coated PCL fibers were observed. Single braiding of a gel-coated PCL mat was achieved with no complications. This was performed immediately after removing the mat from the gelatin bath and carefully drying the surface. At this point, the sample was sufficiently pliable and was easily loaded into the braiding machine (Fig 14A). The braided sample was measured to have a width of 2.3 mm. However, after approximately 30 seconds, the mat began to exhibit extreme brittleness and shattered when manipulated (Fig 14B).

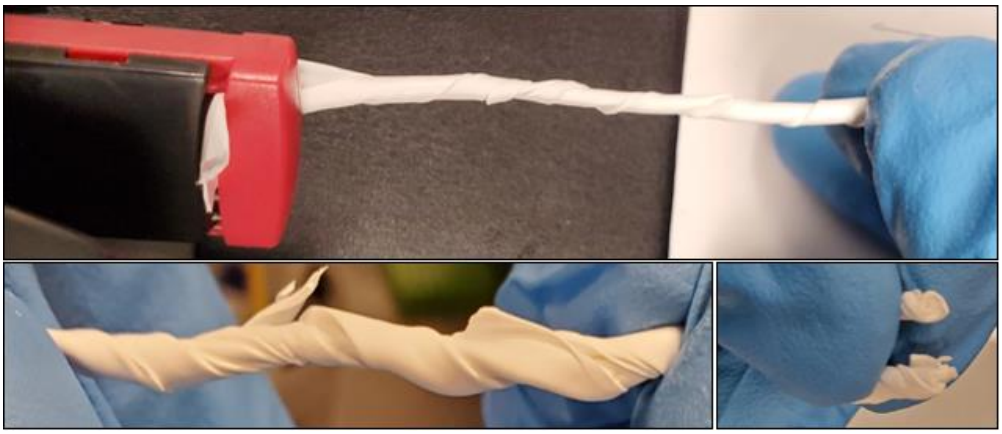

Figure 14: Braided Electrospun PCL fiber mat (A), Braided Electrospun PCL fiber mat after Splintering (B), Broken Braided PCL fiber mat (C)

This loss of elasticity is attributed to the same plasticizing effect noted during tensile testing. The surface gelatin quickly dries when removed from the coating bath and forms thin sheets of biopolymer that fissure when rotation force is applied during braiding (CITE). This made double braiding and tensile testing of the braided samples impossible as the large samples would splinter when loaded into the tensile testing machine, thus the target width of 8.3 mm and tensile data was not obtained for the braided fiber scaffolds. Future work could attempt to amend this issue either by incorporating gelatin into the fiber solution during electrospinning or by attempting stacked braiding of thin (~500 μm) fiber sheets as described in other studies (Rothruaff 2017).

Enzyme Degradation

The eventual goal for these polymer scaffolds is to be used in vivo as knee ligament prosthetics. As such, it is necessary to ensure that the prototypes developed are capable of functioning inside the hostile, enzyme rich environment of the knee long enough for new cell growth to occur on the fiber scaffold. It has been established (Fu 2014) that cell growth on

gelatin/PCL tissue scaffolds platues after seven days of culture time. As uncoated PCL has been shown to resist hydrolytic biodegradation in PBS for up to 50 days (Diaz-Gomez 2014), an incubation of period of five days was arranged to offer insight into the degradation tendency of the gelatin-coated PCL fibers. A trial of only phosphate buffered saline (PBS) was performed to serve as a point of comparison to the enzyme trials. Samples were prepared and their mass was measured over the course of five days.

Table 6: Mass loss of Gelatin Coated PCL scaffold samples over five days incubation in PBS

Degradation Trial 1: Phosphate Buffered Saline					
Sample Number	**Day 0 Mass (dry) (mg)**	**Day 1 Mass (mg)**	**Mass Day 3 (mg)**	**Mass Day 5 (mg)**	**Average Mass Loss (%)**
1	3.1	6.7	5.6	4.6	21.20%
2	3.0	6.5	6.1	4.9	
3	2.1	4.5	4.5	4.1	
4	3.0	7.5	7.2	5.7	
5	2.7	7.0	6.9	5.8	

Table 6 serves as the control for the enzyme studies. It documents the degradation of gelatin-coated PCL samples during hydrolytic degradation via the phosphate buffered saline (PBS) enzyme medium. In the table, the data suggests that that there is initially no major change in sample mass over the first three days. However, there is a noticeable drop in sample mass at the five-day mark. This is attributed to ionic group interaction between the PBS and the gelatin coating the PCL. This likeness in polarity suggests that the primary contributor to mass loss is the solvation of the gelatin coating on the PCL surface over time.

Table 7: Mass loss of Gelatin Coated PCL scaffold samples over five days incubation in PBS+Collagenase (250 µg/mL)

Degradation Trial 2: MMP-1 Collagenase (250 µg/mL)					
Sample Number	**Day 0 Mass (dry) (mg)**	**Day 1 Mass (mg)**	**Mass Day 3 (mg)**	**Mass Day 5 (mg)**	**Average Mass Loss (%)**
1	3.2	8.0	7.2	6.4	15.95%
2	3.0	7.7	6.9	6.3	
3	2.5	5.8	4.9	4.7	
4	2.3	6.9	6.7	6.3	
5	2.2	6.6	5.8	5.3	
6	2.1	6.0	5.9	4.9	

Table 7 shows the degradation of the PCL/Gel samples in the presence of MMP-1. MMP-1 is a collagenase enzyme. Gelatin is a hydrolyzed form of collagen composed of MMP-1-sensitive degradation sites (Suvarnapathaki 2019), so degradation of the gelatin surface was expected in this step. This study shows a gradual degradation to a lesser degree compared to the control trial with a average mass loss of about 16%. One explanation for this outcome is that the MMP-1-sensitive sites on the gelatin become saturated during incubation and thus the degradation occurs at a slower pace than PBS medium alone.

Table 8: Mass loss of Gelatin Coated PCL scaffold samples over five days incubation in PBS+Elastase (100 µg/mL)

Degradation Trial 3: Elastase (100 µg/mL)					
Sample Number	**Day 0 Mass (dry) (mg)**	**Day 1 Mass (mg)**	**Mass Day 3 (mg)**	**Mass Day 5 (mg)**	**Average Mass Loss (%)**
1	2.2	6.6	6.6	6.4	14.59%
2	2.2	6.5	6.4	5.4	
3	3.4	8.6	7.2	6.3	
4	2.0	4.8	4.8	4.7	
5	2.9	7.2	5.4	4.8	
6	2.1	5.5	5.5	5.2	

The elastase trial tabulated above in Table 8 shows mixed results. Samples 1, 4 and 6 show only minor changes over the course of the 5-day period. Other samples degraded consistently, losing over 1 milligram of mass every two days. Such results suggest that the

PCL/Gel scaffolds remain structurally sound over the course of week with small but still apparent changes in mass. Elastase is a serine protease that degrades proteins by cleaving peptide bonds. Specifically, elastase-like proteases tend to prefer small to medium sized hydrophobic amino acid substrates such as alanine or valine (Ovaere 2009) which make up about 11.96% of the amino acid content of bovine gelatin (Gauza 2017). It is possible that the relatively low amount of amino acid substates for elastase degradation results in a small loss of sample mass over five days.

CHAPTER IV

CONCLUSIONS

Polycaprolactone was successfully synthesized from ε -caprolactone via ring-opening polymerization using a stannous octoate catalyst. PCL microfiber scaffolds were successfully fabricated by electrospinning and coated with gelatin via a hot-bath application. These fibers were confirmed to show good distribution, porosity, and even gelatin coating as illustrated by scanning electron microscopy. During tensile testing, unaligned PCL fibers showed good tensile strength but lacked the resistance to elongation and were mechanically inconsistent overall. This was attributed to restricted molecule mobility due to lack of fiber alignment. Thinner fiber mat samples with better fiber alignment fared better, demonstrating Young's Modulus values that represented good elasticity due to better fiber chain elongation during alignment. Aligned-fiber gelatin coated scaffolds produced favorable results during mechanical testing. Tensile testing for gelatin coated aligned fibers showed good physical properties with a mean Young's Modulus measurement over 120 MPa indicating a good stress and strain relationship. This suggests the gelatin coated fiber mats are good potential tissue scaffold prototypes with regards to the mechanical demands of the ACL. Braiding of the PCL/Gel scaffolds was not achieved due to the surface-coated gelatin drying and shattering during the twisting process. It was hypothesized that in the future, electrospinning the gelatin with the PCL solution could circumvent this issue due to better incorporation into the microfiber structure. Also, different methods of fiber sample braiding could produce smaller, more easily characterizable braided PCL mats.

As the long-term goal of this project is to fabricate a sample that can serve in the same capacity as the anterior cruciate ligament, there were attempts to determine the biochemical characteristics of the polymer samples. Enzyme degradation studies were carried out to determine to what degree the polymer microfiber scaffold would break down in a simulated synovial fluid environment of the knee. These trials found that the gelatin-coated PCL scaffolds degraded moderately in the presence of PBS alone like due to solvation of gelatin across the entire PCL surface resulting in mass loss over 20% over five days. In the presence of MMP-1 collagenase, mass loss occurred at a consistent rate likely due to the presence of MMP-1-sensitive sites on the surface of gelatin. High concentrations of elastase resulted in the smallest degree of gelatin-coated PCL fibers degradation. This was attributed to a relatively low substrate content of bovine gelatin. These results suggest that these polymer tissue scaffolds degrade at a consistent pace with no severe degradation in the time necessary for cell proliferation and neoligamentization.

Future investigations into the potential of this material in the field of tissue engineering and specifically knee ligament arthroplasty are wide ranging. There are many variations of PCL/copolymer electrospinning that have yet to be fully explored. Methods for improving the physical properties of the microfiber scaffold via braiding can be developed. Once the tensile characteristics are more favorable, investigation into the biocompatibility of such scaffolds could follow to determine the degree of ease for generation of new tissue such as blood vessels along a PCL scaffold.

REFERENCES

Albertsson, A.-C.; Varma, I. K. Recent Developments in Ring Opening Polymerization of Lactones for Biomedical Applications. *Biomacromolecules* 2003, *4* (6), 1466–1486.

Cimino, F.; Volk, B. S.; Setter, D. Anterior Cruciate Ligament Injury: Diagnosis, Management, and Prevention. *Am. Fam. Physician* 2010, *82* (8), 917–922.

Cramariuc, B.; Cramariuc, R.; Scarlet, R.; Manea, L. R.; Lupu, I. G.; Cramariuc, O. Fiber Diameter in Electrospinning Process. *J. Electrostat*. 2013, *71* (3), 189–198.

Diaz-Gomez, L.; Alvarez-Lorenzo, C.; Concheiro, A.; Silva, M.; Dominguez, F.; Sheikh, F. A.; Cantu, T.; Desai, R.; Garcia, V. L.; Macossay, J. Biodegradable Electrospun Nanofibers Coated with Platelet-Rich Plasma for Cell Adhesion and Proliferation. *Mater. Sci. Eng. C Mater. Biol. Appl*. 2014, *40*, 180–188.

DiFelice, G. S.; Villegas, C.; Taylor, S. Anterior Cruciate Ligament Preservation: Early Results of a Novel Arthroscopic Technique for Suture Anchor Primary Anterior Cruciate Ligament Repair. *Arthroscopy* 2015, *31* (11), 2162–2171.

Doshi, J.; Reneker, D. H. Electrospinning Process and Applications of Electrospun Fibers. *J. Electrostat*. 1995, *35* (2–3), 151–160.

Dou, L.; Li, B.; Zhang, K.; Chu, X.; Hou, H. Physical Properties and Antioxidant Activity of Gelatin-Sodium Alginate Edible Films with Tea Polyphenols. *Int. J. Biol. Macromol.* 2018, *118*, 1377–1383.

Feng, B.; Tu, H.; Yuan, H.; Peng, H.; Zhang, Y. Acetic-Acid-Mediated Miscibility toward

Electrospinning Homogeneous Composite Nanofibers of GT/PCL. *Biomacromolecules* 2012, *13* (12), 3917–3925.

Filatov, Y.; Budyka, A.; Kirichenko, V. N. *Electrospinning of Micro- and Nanofibers: Fundamentals in Separation and Filtration Processes*; Begell House, 2007.

Fong, H.; Chun, I.; Reneker, D. H. Beaded Nanofibers Formed during Electrospinning. *Polymer (Guildf.)* 1999, *40* (16), 4585–4592.

Fu, W.; Liu, Z.; Feng, B.; Hu, R.; He, X.; Wang, H.; Yin, M.; Huang, H.; Zhang, H.; Wang, W. Electrospun Gelatin/PCL and Collagen/PLCL Scaffolds for Vascular Tissue Engineering. *Int. J. Nanomedicine* 2014, *9*, 2335–2344.

Gauza-Włodarczyk, M.; Kubisz, L.; Włodarczyk, D. Amino Acid Composition in Determination of Collagen Origin and Assessment of Physical Factors Effects. *Int. J. Biol. Macromol.* 2017, *104* (Pt A), 987–991.

Gentile, P.; Chiono, V.; Carmagnola, I.; Hatton, P. V. An Overview of Poly(Lactic-Co-Glycolic) Acid (PLGA)-Based Biomaterials for Bone Tissue Engineering. *Int. J. Mol. Sci*. 2014, *15* (3), 3640–3659.

Ginestra, P.; Ceretti, E.; Fiorentino, A. Electrospinning of Poly-Caprolactone for Scaffold Manufacturing: Experimental Investigation on the Process Parameters Influence. *Procedia CIRP* 2016, *49*, 8–13.

Girgis, F. G.; Marshall, J. L.; Mona Jem, A. R. S. A. The Cruciate Ligaments of the Knee Joint: Anatomical. Functional and Experimental Analysis. *Clin. Orthop. Relat. Res.* 1975, *106*, 216–231.

Gorodzha S.N., Surmeneva M.A., Surmenev R.A., Fabrication and Characterization of Polycaprolactone Cross-Linked and Highly-Aligned 3-D Artificial Scaffolds for Bone Tissue Regeneration via Electrospinning Technology. Nanobiotech IOP Conf. Series. 2015, *98* (012024).

Hoogenboom, R.; Schubert, U. S. Microwave-Assisted Polymer Synthesis: Recent Developments in a Rapidly Expanding Field of Research. *Macromol. Rapid Commun.* 2007, *28* (4), 368–386.

Jeong, S. I.; Kim, S. H.; Kim, Y. H.; Jung, Y.; Kwon, J. H.; Kim, B.-S.; Lee, Y. M. Manufacture of Elastic Biodegradable PLCL Scaffolds for Mechano-Active Vascular Tissue Engineering. *J. Biomater. Sci. Polym. Ed.* 2004, *15* (5), 645–660.

Kanjwal, M. A.; Sheikh, F. A.; Nirmala, R.; Macossay, J.; Kim, H. Y. Fabrication of Poly(Caprolactone) Nanofibers Containing Hydroxyapatite Nanoparticles and Their Mineralization in a Simulated Body Fluid. *Fiber. Polym.* 2011, *12* (1), 50–56.

Khokhlov, A. R. High Elasticity of Polymer Networks, 2009. Polymer Physics Dept. Moscow State University. Web site. http://polly.phys.msu.ru/en/education/courses/polymer-intro/lecture3.pdf (Accessed Nov 18, 2021)

Kricheldorf, H. R.; Behnken, G.; Schwarz, G. Ultra-High Molecular Weight Poly(ε-Caprolactone) by Means of Diphenyl Bismuth Bromide. *J. Polym. Sci. A Polym. Chem.* 2008, *46* (3), 851–859.

Lee, S. H.; Petersilge, C. A.; Trudell, D. J.; Haghighi, P.; Resnick, D. L. Extrasynovial Spaces of the Cruciate Ligaments: Anatomy, MR Imaging, and Diagnostic Implications. *AJR Am. J. Roentgenol.* 1996, *166* (6), 1433–1437.

Liljensten, E.; Gisselfält, K.; Edberg, B.; Bertilsson, H.; Flodin, P.; Nilsson, A.; Lindahl, A.; Peterson, L. Studies of Polyurethane Urea bands for ACL reconstruction. *J. Mater. Sci. Mater. Med.* 2002, *13* (4), 351–359.

Macossay, J.; Sheikh, F. A.; Cantu, T.; Eubanks, T. M.; Salinas, M. E.; Farhangi, C. S.; Ahmad, H.; Hassan, M. S.; Khil, M.-S.; Maffi, S. K.; Kim, H.; Bowlin, G. L. Imaging, Spectroscopic, Mechanical and Biocompatibility Studies of Electrospun Tecoflex® EG 80A Nanofibers and Composites Thereof Containing Multiwalled Carbon Nanotubes. *Appl. Surf. Sci.* 2014, *321*, 205–213.

Maeda, S.; Sawai, T.; Uzuki, M.; Takahashi, Y.; Omoto, H.; Seki, M.; Sakurai, M.

Determination of Interstitial Collagenase (MMP-1) in Patients with Rheumatoid Arthritis. *Ann. Rheum. Dis*. 1995, *54* (12), 970–975.

Mojarad, B.; Torkaman, R.; Mahmoudi, M.; Emadi, R.; Karamian, E. An Improvement in Corrosion Resistance of 316L AISI Coated Using PCL-Gelatin Composite by Dip-Coating Method. *Prog. Org. Coat*. 2019, *130*, 200–205.

Morales, J. O.; McConville, J. T. Manufacture and Characterization of Mucoadhesive Buccal Films. *Eur. J. Pharm. Biopharm*. 2011, *77* (2), 187–199.

Mori, C. L. S. de O.; dos Passos, N. A.; Oliveira, J. E.; Altoé, T. F.; Mori, F. A.; Mattoso, L. H. C.; Scolforo, J. R.; Tonoli, G. H. D. Nanostructured Polylactic Acid/Candeia Essential Oil Mats Obtained by Electrospinning. *J. Nanomater*. 2015, *2015* (4), 1–9.

Obregon, N. MICROWAVE-ASSISTED RING-OPENING POLYMERIZATION OF POLY(ϵ-CAPROLACTONE), The University of Texas Rio Grande Valley, Edinburg, TX, 2018.

Ovaere, P.; Lippens, S.; Vandenabeele, P.; Declercq, W. The Emerging Roles of Serine Protease Cascades in the Epidermis. *Trends Biochem. Sci*. 2009, *34* (9), 453–463.

Palmer, M.; Stanford, E.; Murray, M. M. The Effect of Synovial Fluid Enzymes on the Biodegradability of Collagen and Fibrin Clots. *Materials (Basel)* 2011, *4* (8), 1469–1482.

Pauly, H.; Kelly, D.; Popat, K.; Easley, J.; Palmer, R.; Haut Donahue, T. L. Mechanical Properties of a Hierarchical Electrospun Scaffold for Ovine Anterior Cruciate Ligament Replacement: MECHANICAL PROPERTIES OF IMPLANTED ACL SCAFFOLD. *J. Orthop. Res.* 2019, *37* (2), 421–430.

Peeler, J.; Anderson, J.; Piotrowski, S.; Stranges, G. Motion of the Anterior Cruciate Ligament during Internal and External Rotation at the Knee: A Cadaveric Study. *Clin. Anat*. 2017, *30* (7), 861–867.

Pham, Q. P.; Sharma, U.; Mikos, A. G. Electrospinning of Polymeric Nanofibers for Tissue Engineering Applications: A Review. *Tissue Eng*. 2006, *12* (5), 1197–1211.

Polymer Properties Database: Strain Hardening of Amorphous and Semi-Crystalline Polymers https://polymerdatabase.com/polymer%20physics/Strain%20Hardening.html (accessed Oct 23, 2021).

Sayyar, S.; Murray, E.; Thompson, B. C.; Gambhir, S.; Officer, D. L.; Wallace, G. G. Covalently Linked Biocompatible Graphene/Polycaprolactone Composites for Tissue Engineering. *Carbon N. Y.* 2013, *52*, 296–304.

Seidman, A. J.; Limaiem, F. Synovial Fluid Analysis. NCBI Web site. *StatPearls Pub.* 2021,

Sheng, D.; Li, J.; Ai, C.; Feng, S.; Ying, T.; Liu, X.; Cai, J.; Ding, X.; Jin, W.; Xu, H.; Chen, J.; Chen, S. Electrospun PCL/Gel-Aligned Scaffolds Enhance the Biomechanical Strength in Tendon Repair. *J. Mater. Chem. B Mater. Biol. Med.* 2019, *7* (31), 4801–4810.

SpecialChem. Polymer Properties: Elongation at Break https://omnexus.specialchem.com/polymer-properties (accessed Oct 2, 2021).

Spindler, K. P.; Wright, R. W. Clinical Practice. Anterior Cruciate Ligament Tear. *N. Engl. J. Med.* 2008, *359* (20), 2135–2142.

Suvarnapathaki, S.; Nguyen, M. A.; Wu, X.; Nukavarapu, S. P.; Camci-Unal, G. Synthesis and Characterization of Photocrosslinkable Hydrogels from Bovine Skin Gelatin. *RSC Advances* 2019, *9* (23), 13016–13025.

Tchetverikov, I.; Lohmander, L. S.; Verzijl, N.; Huizinga, T. W. J.; TeKoppele, J. M.; Hanemaaijer, R.; DeGroot, J. MMP Protein and Activity Levels in Synovial Fluid from Patients with Joint Injury, Inflammatory Arthritis, and Osteoarthritis. *Ann. Rheum. Dis.* 2005, *64* (5), 694–698.

van Zyl, R.; van Schoor, A.-N.; du Toit, P. J.; Louw, E. M. Clinical Anatomy of the Anterior Cruciate Ligament and Pre-Operative Prediction of Ligament Length. *SA Orthop.*

J. 2016, *15* (4). https://doi.org/10.17159/2309-8309/2016/v15n4a7.

Wright, L. D.; Andric, T.; Freeman, J. W. Utilizing NaCl to Increase the Porosity of Electrospun Materials. Mater. Sci. Eng. C Mater. *Biol. Appl*. 2011, *31* (1), 30–36.

BIOGRAPHICAL SKETCH

Diego Rivera was born in Corpus Christi, Texas on December 28, 1995. He grew up primarily in Falfurrias, Texas and graduated from Falfurrias High School in 2014. Afterwards, he continued his education at the University of Texas Rio Grande Valley (then known as the University of Texas Pan American). He joined the Ateşin Organometallic Chemistry research group in 2015 and worked on various joint projects focused on molecular confirmation analysis of palladium-catalyzed reactions. This work has been published in journals such as Computational and Theoretical Chemistry and the Journal of Organic Chemistry. After graduating with his bachelor's degree in chemistry in 2018, Diego continued his education at UTRGV to obtain his master's degree in chemistry. Diego joined the Macossay Polymer Chemistry research group in 2019 studying materials with potential for biomedical applications. During both his undergraduate and graduate programs, Diego worked as a chemistry tutor, laboratory teaching assistant, and eventually a graduate teaching assistant in a variety of laboratories for the chemistry department at UTRGV. He obtained his master's degree in chemistry from UTRGV in December of 2021.

Permanent mailing address: 2625 Northgate Ln, McAllen, TX 78504

Author's personal email address: d.rivera7034@gmail.com